Poloidally asymmetric emission of visible light in RTP

Poloidally asymmetric emission of visible light in RTP

L.C. Ingesson, A.J.H. Donné, D.C. Schram* and RTP-team

FOM-Instituut voor Plasmafysica "Rijnhuizen", Associatie Euratom-FOM, P.O. Box 1207, 3430 BE Nieuwegein, The Netherlands
*Technische Universiteit Eindhoven, P.O. Box 513, 5600 MB Eindhoven, The Netherlands

Introduction

Virtually all poloidal emission profiles measured by the 80-channel visible-light tomography system on RTP are asymmetric. Measurements in three spectral ranges are presented: the H_α-line (656 nm), the range 695 – 1100 nm (to measure continuum radiation), and the total range 300 – 1100 nm to which the detectors are sensitive. From the emissivity the local neutral hydrogen density is calculated. The continuum measurements have been used to derive the effective ionic charge Z_{eff} in the plasma centre, the determination of which is affected by asymmetries at the edge. Possible causes for the asymmetrical emission at the edge are discussed.

The visible-light tomography system and its calibration

The emitted visible light is collected from five viewing directions in one poloidal cross-section by optical imaging systems, each with 16 detectors [1]. The viewing chords were chosen to cover mainly the edge of the plasma (where most visible light is emitted) and were largely determined by the limited access to the tokamak vessel. The resulting coverage consists of five partial views of the plasma, together viewing virtually each part of plasma from at least two directions.

The geometrical properties of the system have been determined to account for imaging, chord-width, vignetting, detector sensitivity and reflections on the walls (most parts, but not all, are covered by viewing dumps). The central wavelength and the transmission of interference filters depend on the angles of incidence, which are rather large in this system due to the optical imaging system and which vary for the different detectors on the array (between 10° and 16°). Therefore, a correction between channels of several percent is needed for the transmission of the H_α filters used, despite their relatively large full-width-half-maximum of 10 nm [2]. The magnitude of the correction depends sensitively on the central wavelength of the filter. Furthermore, for non-normal incidence the peak transmission decreases, which cannot be neglected. To collect a sufficient amount of light in the continuum measurements an optical filter with a large bandwidth is used instead of a narrow filter for a line-free part of the spectrum. For this purpose a sharp cutoff coloured-glass filter is applied, which transmits wavelengths longer than 695 nm. Due to the spectral dependence of the detector sensitivity, an absolute calibration is only easily obtained if the spectral emissivity is independent of frequency. This is a good approximation for Bremsstrahlung in the visible range at electron temperatures $T_e > 100$ eV, i.e. everywhere in the plasma except at the edge.

The application of two tomography algorithms

Two different tomography methods are used, which are designated as method A and method B. Method A [3] was developed specifically for the visible-light tomography system. The iterative algorithm interpolates the line-integrated signals from the non-uniformly distributed lines-of-sight of the system to what would be measured by regularly distributed lines-of-sight, taking into account *a priori* information (such as smoothness, boundary conditions and consistency of the tomographic reconstruction). The properties of the imaging system are taken into account by scaling the measurements to the signals expected for line integrals. In method B [4] the tomography problem is discretized and the local emissivity is obtained by optimizing the solution of an underdetermined set of linear equations, describing the geometric properties of the system. In the optimization, smoothness is imposed and the experimental level of noise is taken into account.

Numerical simulations and reconstructions of measurements have shown that for symmetrical peaked and hollow profiles both methods produce good results. Due to uncertainties in the imaging properties of the system at the plasma edge, reconstructions of emission profiles with appreciable radiation from outside the plasma region are of lesser quality. In general the performance of the two tomography methods can be summarized as follows: method A oversmooths the result, in particular localized peaks of emissivity; method B gives reliable reconstructions, but it sometimes yields unrealistically high emissivities at the edge due to uncertainties in system characteristics. For the highly asymmetric profiles the results of the methods may differ, which is an indication that the coverage of the system is insufficient to completely determine the emission profile. Comparison of the two methods, however, can show which parts of the reconstructed emission profiles are reliable, making it possible to determine approximate absolute emissivity values.

H_α measurements

Tomographic reconstructions by both methods of the H_α emission during a 90 kA Ohmic discharge with peak electron density $n_e = 5 \times 10^{19}\ m^{-3}$ and temperature $T_e = 1$ keV are shown in Figs. 1(a) and 1(b). The shape of the H_α emission profile is roughly the same for most plasma conditions; only the magnitude varies roughly proportionally to n_e. If, however, the plasma is moved or the direction of the toroidal magnetic field is reversed, the positions of the asymmetric peaks change significantly. The thickness of the radiating layer at the edge is about

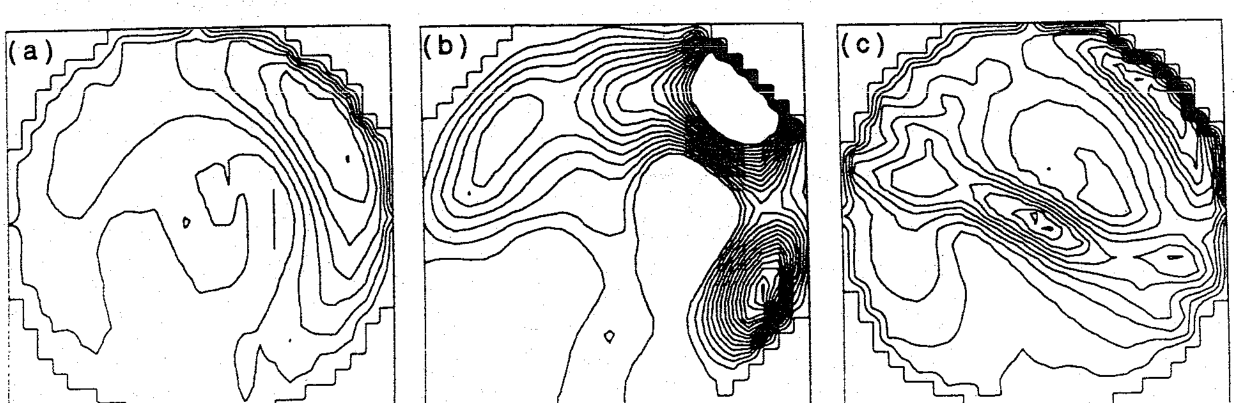

Fig. 1 Tomographic reconstructions of H_α emission by (a) method A and (b) method B. Each contour represents 2 $W\ m^{-3}\ sr^{-1}$. (c) Tomographic reconstruction by method A of continuum radiation. Each contour represents $2 \times 10^{-15}\ W\ m^{-3}\ sr^{-1}\ Hz^{-1}$. The reconstruction area has a radius of 0.190 m, outside which zero emission is assumed (the minor radius of the limiter in RTP is 0.165 m). The area shown is $0.38 \times 0.38\ m^2$ centred around the centre of the vacuum vessel. The high-field side is on the left.

4 cm [of which 2 cm in the scrape-off layer (SOL)], which roughly corresponds to the penetration length of neutrals under the influence of ionization and charge-exchange.

An estimate from the tomographic reconstructions of the peak emissivity in the main asymmetry is 20 W sr^{-1} m^{-3} for this discharge. The emissivity outside the main peak ranges from 5 to 10 W sr^{-1} m^{-3}. The main peak radiates about 40% to 60% of the total H_α power in the poloidal cross-section. The H_α emissivity is proportional to the population density of level $n = 3$ in hydrogen, where n is the principal quantum number. The ground state density level can be related to this population density by calculations with the collisional-radiative model of Johnson and Hinnov [5]. From this analysis the neutral hydrogen density, which is approximately equal to the ground state density, of $4 \times 10^{16}\,m^{-3}$ in the main peak is found. Opacity of the Lyman lines does not play a role at these densities. This value is fairly independent of variations in n_e and T_e.

In the above calculations only excitation of atomic hydrogen by electronic collisions has been taken into account. Excited atomic hydrogen, however, also results from various dissociative processes of H_2^+, in particular dissociative ionization. Taking these processes into account [6] changes the results, but not significantly. However, a significant fraction of the excited hydrogen atoms results from the H_2^+ ions, which have an estimated lifetime of 10^{-4} to 10^{-5} s. Therefore, the location of the H_α emission can be significantly affected by the fast transport of ions along the field lines. This is further discussed in the paragraph about poloidal asymmetries.

Continuum measurements

Figure 1(c) shows a tomographic reconstruction by method A of the emission profile measured with the continuum filter. The Bremsstrahlung in the visible range is proportional to n_e^2, $\sqrt{1/T_e}$ and Z_{eff}. For this discharge the emissivity in the centre corresponds to $Z_{eff} = 4 \pm 1$, which is higher than $Z_{eff} \approx 2$ as determined from Spitzer resistivity. By comparing the line-integrated measurements with the calculated Bremsstrahlung profile for which Z_{eff} is assumed to be constant over the cross-section, the channels measuring the least signal (i.e. not affected much by the edge emission) indicate that Z_{eff} cannot be higher than 3. The Z_{eff} found from the reconstruction of the continuum radiation is reasonable despite the presence of artefacts in the tomographic reconstruction (hollow areas in the plasma where reconstructed emissivities are smaller than expected for Bremsstrahlung) that result from the large asymmetries at the edge. The radiation from the edge is probably due to molecular radiation from H_2 and possibly line radiation from light impurities, but no spectral overview is available of the observed spectral range to verify this. Of the total emissivity over the cross-section measured with the continuum filter, only 10% to 40% can be accounted for by Bremsstrahlung

Comparison of contributions to the total emitted visible light

The amount of radiation emitted in the different measured wavelength ranges can be compared with the total emitted visible light. If the signal level measured with the continuum filter is extrapolated to the entire wavelength range, it is found that the contribution of H_α is roughly two times that of the extrapolated continuum radiation, and that the measured H_α radiation and the extrapolated continuum radiation together approximately account for the total measured radiation. There is, however, a large variation in signal levels between discharges. Because only a minor part of the radiation measured with the continuum filter is Bremsstrahlung, the extrapolation to the total range is rather rough. However, because the extrapolation yields approximately the total measured radiation, it can be concluded that the contribution from radiation other than H_α and Bremsstrahlung is approximately of the same level for all wavelengths.

Discussion on asymmetries and conclusions

In the literature both poloidal and toroidal asymmetries of the emission profiles of H_α and light impurities have been reported [7]. It has been suggested [8] that the asymmetries of emission from impurities and hydrogen are related to the $\boldsymbol{B} \times \nabla \boldsymbol{B}$ drift of ions. Indeed, in RTP the positions change when the field is reversed, but not in a symmetrical way, indicating that at least other effects play a role as well. Because the asymmetric peaks in emission occur mainly on the low-field side and are present in virtually all discharges, these are not likely to be marfes. Although H_2^+ ions produced at the limiter can explain an asymmetry in the H_α emission at other positions than the recycling location because they flow along the field lines, and the fact that asymmetries change position when the plasma column is moved, the positions of the asymmetries do not seem related in a clear way to the limiter and the field lines. Detailed studies with relatively high-resolution tomography systems such as the one on RTP can give more insight in the magnitude of the asymmetric peaks. However, due to the profound asymmetries the coverage of the system at RTP is only sufficient to resolve the major features. An improved coverage would decrease the artefacts and would therefore enable an even better determination of the Bremsstrahlung and Z_{eff} in the centre. For a better understanding of the asymmetries more edge diagnostic data and more spectroscopic information would be advantageous.

The asymmetries resolved by visible light tomography, albeit found in a small tokamak on which the asymmetries are expected to be relatively large due to the relatively thick edge and scrape-of-layer, suggest the need for a more careful evaluation of spectral measurements and of the applicability of Abel inversion on multi-chord data on other tokamaks.

Acknowledgements

We are grateful to G.C. Fehmers for providing us with his tomographic inversion code, and to Dr. V.V. Pickalov for the collaboration on developing a new tomographic inversion method suitable for our tomography system. We thank Prof. F.C. Schüller for the stimulating discussions about this paper. This work was done under the Euratom-FOM association agreement with financial support from NWO and Euratom.

References

[1] L.C. Ingesson *et al.*, Rev. Sci. Instrum. **63**, 5185 (1992)
[2] L.C. Ingesson *et al.*, Rev. Sci. Instrum. **66**, 622 (1995)
[3] V.V. Pickalov *et al.*, Proc. 1992 Int. Conf. on Plasma Physics, Innsbruck, Part II, p. 1143
[4] G.C. Fehmers, to be published.
[5] L.C. Johnson, E. Hinnov, J. Quant. Spectrosc. Radiat. Transfer **13**, 333 (1973)
[6] D.H. McNeill *et al.*, J. Vac. Sci. Technol. A **2**, 689 (1984)
[7] R.C. Isler, Nucl. Fusion **24**, 1599 (1984)
[8] K. Brau *et al.*, Nucl. Fusion **23**, 1657 (1983)